

## Symmetry Control of Radiative Decay in Linear Polyenes: Low Barriers for Isomerization in the S<sub>1</sub> State of Hexadecaheptaene

Ronald L. Christensen,<sup>\*,†</sup> Mary Grace I. Galinato,<sup>‡</sup> Emily F. Chu,<sup>‡</sup> Ritsuko Fujii,<sup>§</sup>  
Hideki Hashimoto,<sup>||</sup> and Harry A. Frank<sup>\*,‡</sup>

Contribution from the Department of Chemistry, Bowdoin College,  
Brunswick, Maine 04011-8466, Department of Chemistry, 55 North Eagleville Road, University  
of Connecticut, Storrs, Connecticut 06269-3060, Department of Physics, Osaka City University,  
3-3-138 Sugimoto, Sumiyoshi-ku, Osaka 558-8585, Japan, and "Light and Control"  
PRESTO/JST, 4-1-8 Honcho Kawaguchi, Saitama 332-0012, Japan

Received February 9, 2006; E-mail: rchriste@bowdoin.edu; harry.frank@uconn.edu

**Abstract:** The room temperature absorption and emission spectra of the 4-*cis* and *all-trans* isomers of 2,4,6,8,10,12,14-hexadecaheptaene are almost identical, exhibiting the characteristic dual emissions S<sub>1</sub>→S<sub>0</sub> (2<sup>1</sup>A<sub>g</sub><sup>-</sup> → 1<sup>1</sup>A<sub>g</sub><sup>-</sup>) and S<sub>2</sub>→S<sub>0</sub> (1<sup>1</sup>B<sub>u</sub><sup>+</sup> → 1<sup>1</sup>A<sub>g</sub><sup>-</sup>) noted in previous studies of intermediate length polyenes and carotenoids. The ratio of the S<sub>1</sub>→S<sub>0</sub> and S<sub>2</sub>→S<sub>0</sub> emission yields for the *cis* isomer increases by a factor of ~15 upon cooling to 77 K in *n*-pentadecane. In contrast, for the *trans* isomer this ratio shows a 2-fold decrease with decreasing temperature. These results suggest a low barrier for conversion between the 4-*cis* and *all-trans* isomers in the S<sub>1</sub> state. At 77 K, the *cis* isomer cannot convert to the more stable *all-trans* isomer in the 2<sup>1</sup>A<sub>g</sub><sup>-</sup> state, resulting in the striking increase in its S<sub>1</sub>→S<sub>0</sub> fluorescence. These experiments imply that the S<sub>1</sub> states of longer polyenes have local energy minima, corresponding to a range of conformations and isomers, separated by relatively low (2–4 kcal) barriers. Steady state and time-resolved optical measurements on the S<sub>1</sub> states in solution thus may sample a distribution of conformers and geometric isomers, even for samples represented by a single, dominant ground state structure. Complex S<sub>1</sub> potential energy surfaces may help explain the complicated S<sub>2</sub>→S<sub>1</sub> relaxation kinetics of many carotenoids. The finding that fluorescence from linear polyenes is so strongly dependent on molecular symmetry requires a reevaluation of the literature on the radiative properties of *all-trans* polyenes and carotenoids.

### Introduction

The optical spectroscopy of short, *all-trans* polyenes reveals an excited 2<sup>1</sup>A<sub>g</sub><sup>-</sup> singlet state, into which absorption is forbidden by symmetry, lying at lower energy than the 1<sup>1</sup>B<sub>u</sub><sup>+</sup> state responsible for the characteristic strong visible absorption (S<sub>0</sub> (1<sup>1</sup>A<sub>g</sub><sup>-</sup>) → S<sub>2</sub> (1<sup>1</sup>B<sub>u</sub><sup>+</sup>)) in these C<sub>2h</sub> symmetric, linearly conjugated π-electron systems.<sup>1,2</sup> This explains several distinctive aspects of polyene optical spectroscopy, including the systematic differences in the transition energies of the strong absorption and the fluorescence (S<sub>1</sub> (2<sup>1</sup>A<sub>g</sub><sup>-</sup>) → S<sub>0</sub> (1<sup>1</sup>A<sub>g</sub><sup>-</sup>)), the anomalously long radiative lifetimes, and the relative insensitivity of the fluorescence spectra to solvent polarizability.<sup>2</sup> Theoretical analysis by Schulten and Karplus<sup>3</sup> of short, *all-trans* polyenes rationalized the low lying S<sub>1</sub> (2<sup>1</sup>A<sub>g</sub><sup>-</sup>) state in terms of extensive configuration interaction between singly and multiply

excited singlet configurations with the same symmetry. Extensions of this model to longer polyenes and carotenoids predict additional low-lying <sup>1</sup>A<sub>g</sub><sup>-</sup> and <sup>1</sup>B<sub>u</sub><sup>-</sup> excited states,<sup>4,5</sup> but these other states are not easily detected, in either conventional steady-state or time-resolved spectroscopic measurements.

The theoretical descriptions of *all-trans* polyene excited states have had considerable influence, not only in interpreting the spectroscopy and photophysics of *all-trans* polyenes but also in explaining optical measurements on a variety of less symmetric polyenes and carotenoids. For example, Koyama et al.<sup>6,7</sup> assigned features in resonance Raman excitation profiles and in the fluorescence spectra of long carotenoids to low-lying <sup>1</sup>B<sub>u</sub><sup>-</sup> states. This group also used ultrafast optical spectroscopy to detect transient absorption features, again attributed to the <sup>1</sup>B<sub>u</sub><sup>-</sup> state.<sup>8,9</sup> Cerullo et al.<sup>10</sup> presented ultrafast spectroscopic evidence for an intermediate singlet state (S<sub>x</sub>) in several

<sup>†</sup> Bowdoin College.

<sup>‡</sup> University of Connecticut.

<sup>§</sup> Osaka City University.

<sup>||</sup> "Light and Control" PRESTO/JST.

- (1) Hudson, B.; Kohler, B. *Ann. Rev. Phys. Chem.* **1974**, *25*, 437–460.
- (2) Hudson, B. S.; Kohler, B. E.; Schulten, K. Linear polyene electronic structure and potential surfaces. In *Excited States*; Lim, E. D., Ed.; Academic Press: New York, 1982; Vol. 6, pp 1–95.
- (3) Schulten, K.; Karplus, M. *Chem. Phys. Lett.* **1972**, *14*, 305–309.

- (4) Tavan, P.; Schulten, K. *J. Chem. Phys.* **1986**, *85*, 6602–6609.
- (5) Tavan, P.; Schulten, K. *Phys. Rev. B: Condens. Matter* **1987**, *36*, 4337–4358.
- (6) Sashima, T.; Koyama, Y.; Yamada, T.; Hashimoto, H. *J. Phys. Chem. B* **2000**, *104*, 5011–5019.
- (7) Fujii, R.; Onaka, K.; Nagae, H.; Koyama, Y.; Watanabe, Y. *J. Lumin.* **2001**, *92*, 213–222.
- (8) Zhang, J.-P.; Inaba, T.; Watanabe, Y.; Koyama, Y. *Chem. Phys. Lett.* **2000**, *332*, 351–358.

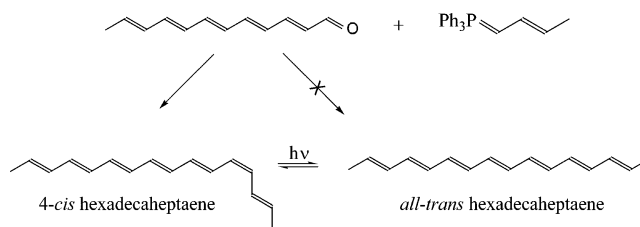
carotenoids, which they postulated facilitates internal conversion between the  $S_2$  ( $1^1B_u^+$ ) and  $S_1$  ( $2^1A_g^-$ ) states. Van Grondelle and co-workers<sup>11</sup> observed a wavelength dependence of the dynamics of spirilloxanthin that was interpreted in terms of another singlet electronic state,  $S^*$ , thought to be an intermediate in the depopulation of  $S_2$  ( $1^1B_u^+$ ). Fast pump–probe optical techniques were applied to  $\beta$ -carotene by Larsen et al.,<sup>12</sup> and the results suggested yet another carotenoid excited state ( $S^\ddagger$ ) formed directly from  $S_2$  ( $1^1B_u^+$ ). The nature of these states remains uncertain, and recent work has called into question the assignments and suggested that at least some of the spectroscopic observations may be attributed to two-photon processes rather than additional electronic states.<sup>13,14</sup>

Advances in synthetic procedures coupled with improved purification and analytical techniques (HPLC, MS/APCI+, and NMR) have allowed us to revisit the electronic states of simple *all-trans* dimethyl polyenes and to extend optical experiments to their less symmetric *cis* counterparts. These studies reveal that the rates of radiative decay from the “ $S_1$  ( $2^1A_g^-$ )” states of *cis* polyenes are significantly larger than radiative decay rates from the  $S_1$  ( $2^1A_g^-$ ) states of *trans* polyenes. Our experiments also suggest that *trans*  $\leftrightarrow$  *cis* conversion readily occurs on the  $S_1$  ( $2^1A_g^-$ ) potential surface. The photochemical formation of *cis* isomers from *trans* ground states requires a reevaluation of previous reports of fluorescence from *trans* polyenes and carotenoids. Many of these studies were carried out prior to the advent of sophisticated high performance liquid chromatography (HPLC) techniques capable of achieving the high level of sample purity and analysis<sup>2,15–27</sup> required to identify the source of fluorescence signals. The work presented here provides an alternate model for internal conversion following the excitation of  $S_2$  ( $1^1B_u^+$ ) and suggests that at least some of the electronic states postulated in recent years may be associated with different geometric isomers and/or conformers formed in the  $S_1$  ( $2^1A_g^-$ ) state. Many of the essential features of the simple

“three state” scheme,  $E(S_2 (1^1B_u^+)) > E(S_1 (2^1A_g^-)) > E(S_0 (1^1A_g^-))$ , are preserved by invoking isomerization and/or conformational change on short time scales in the  $S_1$  ( $2^1A_g^-$ ) state.

## Experimental Section

2,4,6,8,10,12,14-Hexadecaheptaene was synthesized via a Wittig reaction between 2,4,6,8,10,12-dodecapentaenal and crotyltriphenylphosphonium bromide. The hexadecaheptaene products were isolated using silica gel chromatography and then photolyzed to convert the predominantly *cis* mixture into the *all-trans* isomer. HPLC ( $C_{18}$ -reversed phase) was used to isolate the *cis* and *trans* isomers for spectroscopic analysis. Mass spectrometry (MS/APCI+) and NMR spectroscopy (2D  $^1H$ – $^1H$  COSY and NOESY) were used to identify the major product of the Wittig reaction as 4-*cis* hexadecaheptaene. The main photolysis product is the *all-trans* isomer, as summarized in the following reaction scheme:



**Synthesis of 4-*cis*-Hexadecaheptaene.** *All-trans* 2,4,6,8,10,12-dodecapentaenal was obtained by condensing crotonaldehyde (Sigma-Aldrich) as described previously.<sup>19,28,29</sup> 50 mg of the crotyl ylide (Fluka) was combined with 1 mL of anhydrous THF in a 5-mL flask. 17 mg of the dodecapentaenal were added, and the mixture was stirred for 30 min. The characteristic polyene absorption (300–400 nm) was used to follow the buildup of the heptaene product. Aqueous NaOH was added to quench the reaction, and the hexadecaheptaene was extracted using several aliquots of warm hexane. The crude hexadecaheptaene was purified on silica gel (Silica Gel 60-EM Reagents) using hexane as a mobile phase.

**Photoisomerization and High-Performance Liquid Chromatography (HPLC) of Hexadecaheptaene.** Hexadecaheptaene fractions collected from the silica gel column were evaporated and reconstituted in acetonitrile (Fisher Scientific, HPLC-grade) and placed in a 1-cm path length quartz spectrophotometer cell. The sample (absorbance  $\sim 1.6$ ) was exposed to 396 nm light with a 14.7 nm band-pass using a Jobin-Yvon Horiba Fluorolog-3 fluorescence spectrometer (see below). The illumination was interrupted every 5 min to mix the sample and to record the absorption spectrum. The total sample illumination time was 30 min. The photolyzed sample was analyzed using a Waters HPLC equipped with a 600S controller, a 616 pump, and a 717plus autosampler. A Waters 996 photodiode array detector (PDA) monitored the absorption spectra of the peaks as they eluted from a Nova-Pak reversed-phase C18 column (3.9 mm  $\times$  300 mm, 60 Å pore size, and 4  $\mu$ m particle size of spherical amorphous silica). Acetonitrile was used as the mobile phase, and the system was run in isocratic mode at a flow rate of 0.5 mL/min.

**Characterization of Hexadecaheptaene Isomers by Nuclear Magnetic Resonance Spectroscopy.** The dominant isomer in the unphotolyzed hexadecaheptaene sample (Figure 1) was isolated by HPLC using a 250 mm  $\times$  4.6 mm YMC-Pak  $C_{18}$ -A column (5- $\mu$ m particle size, 12-nm pore size) and acetonitrile as the mobile phase. 1D and 2D  $^1H$  NMR spectra, including  $^1H$ – $^1H$  COSY and  $^1H$ – $^1H$  NOESY spectra, were recorded in chloroform- $D$  at room-temperature using a 600 MHz FT NMR spectrometer. Proton signals corresponding

- (9) Koyama, Y.; Rondonuwu, F. S.; Fujii, R.; Watanabe, Y. *Biopolymers* **2004**, *74*, 2–18.
- (10) Cerullo, G.; Polli, D.; Lanzani, G.; De Silvestri, S.; Hashimoto, H.; Cogdell, R. J. *Science* **2002**, *298*, 2395–2398.
- (11) Gradinaru, C. C.; Kennis, J. T. M.; Papagiannakis, E.; van Stokkum, I. H. M.; Cogdell, R. J.; Fleming, G. R.; Niederman, R. A.; van Grondelle, R. *Proc. Natl. Acad. Sci. U.S.A.* **2001**, *98*, 2364–2369.
- (12) Larsen, D. S.; Papagiannakis, E.; van Stokkum, I. H. M.; Vengris, M.; Kennis, J. T. M.; van Grondelle, R. *Chem. Phys. Lett.* **2003**, *381*, 733–742.
- (13) Kukura, P.; McCamant, D. W.; Mathies, R. A. *J. Phys. Chem. A* **2004**, *108*.
- (14) Kosumi, D.; Komukai, M.; Hashimoto, H.; Yoshizawa, M. *Phys. Rev. Lett.* **2005**, *95*, 213601–213604.
- (15) Kohler, B. E.; Terpougov, V. *J. Chem. Phys.* **1998**, *108*, 9586–9593.
- (16) Christensen, R. L.; Kohler, B. E. *J. Phys. Chem.* **1976**, *80*, 2197–2200.
- (17) Christensen, R. L.; Barney, E. A.; Broene, R. D.; Galinato, M. G. I.; Frank, H. A. *Arch. Biochem. Biophys.* **2004**, *430*, 30–36.
- (18) Simpson, J. H.; McLaughlin, L.; Smith, D. S.; Christensen, R. L. *J. Chem. Phys.* **1987**, *87*, 3360–3365.
- (19) Snyder, R.; Arvidson, E.; Foote, C.; Harrigan, L.; Christensen, R. L. *J. Am. Chem. Soc.* **1985**, *107*, 4117–4122.
- (20) Frank, H. A.; Josue, J. S.; Bautista, J. A.; van der Hoef, I.; Jansen, F. J.; Lugtenburg, J.; Wiederrecht, G.; Christensen, R. L. *J. Phys. Chem. B* **2002**, *106*, 2083–2092.
- (21) Shima, S.; Ilagan, R. P.; Gillespie, N.; Sommer, B. J.; Hiller, R. G.; Sharples, F. P.; Frank, H. A.; Birge, R. R. *J. Phys. Chem. A* **2003**, *107*, 8052–8066.
- (22) Fujii, R.; Onaka, K.; Kuki, M.; Koyama, Y.; Watanabe, Y. *Chem. Phys. Lett.* **1998**, *288*, 847–853.
- (23) Josue, J. S.; Frank, H. A. *J. Phys. Chem. A* **2002**, *106*, 4815–4824.
- (24) Frank, H. A.; Bautista, J. A.; Josue, J. S.; Young, A. J. *Biochemistry* **2000**, *39*, 2831–2837.
- (25) Onaka, K.; Fujii, R.; Nagae, H.; Kuki, M.; Koyama, Y.; Watanabe, Y. *Chem. Phys. Lett.* **1999**, *315*, 75–81.
- (26) Andersson, P. O.; Bachilo, S. M.; Chen, R.-L.; Gillbro, T. *J. Phys. Chem.* **1995**, *99*, 16199–16209.
- (27) Auerbach, R. A.; Christensen, R. L.; Granville, M. F.; Kohler, B. E. *J. Chem. Phys.* **1981**, *74*, 4–9.

- (28) D’Amico, K. L.; Manos, C.; Christensen, R. L. *J. Am. Chem. Soc.* **1980**, *102*, 1777–1782.
- (29) Palmer, B.; Jumper, B.; Hagan, W.; Baum, J. C.; Christensen, R. L. *J. Am. Chem. Soc.* **1982**, *104*, 6907–6913.

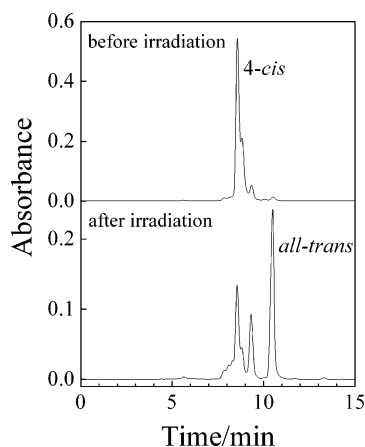


**Figure 1.** HPLC of hexadecaheptaene before and after 396 nm irradiation. Chromatography was done on a  $C_{18}$  reversed phase column using acetonitrile as the mobile phase. Absorbance was monitored at 396 nm.

to the methyl groups showed distinct chemical shifts, indicating an asymmetric structure. Exploiting the 2D correlation peaks starting from the methyl protons, signals due to the ethylenic protons were assigned based on splittings, coupling constants, and COSY cross-peaks between neighboring protons. These assignments are summarized in Figure S1 (Supporting Information). NOE correlations also proved useful in determining the isomeric configuration; e.g., the clear NOE correlation between 3H and 6H confirmed that the 4C=5C bond had a *cis* configuration. Other NOE correlations confirmed *trans* geometries for the other double bonds. The isomer thus was assigned unequivocally as 4-*cis* hexadecaheptaene.

**Fluorescence Spectroscopy.** Individual HPLC peaks were collected, evaporated, and reconstituted in *n*-pentadecane for fluorescence and fluorescence excitation measurements. Samples were reinjected into the HPLC after spectroscopic experiments to verify their isomeric purity after exposure to light. Fluorescence spectra were acquired using a Jobin-Yvon Horiba Fluorolog-3 model FL3-22 spectrometer equipped with double monochromators with 1200 grooves/mm gratings, a Hamamatsu R928P photomultiplier, and a 450 W OSRAM XBO xenon arc lamp. The emission was monitored using front-face detection for the low-temperature experiments and right-angle detection for the room temperature measurements. A home-built, flowing gaseous  $N_2$  quartz cryostat maintained sample temperatures between 77 and 300 K. A gold-chromel thermocouple connected to an Air Products digital temperature controller monitored sample temperatures. For studies of the temperature dependence of fluorescence, purified samples were quickly frozen in liquid nitrogen and then transferred to the flowing  $N_2$  cryostat. The temperature was allowed to equilibrate for several minutes before each spectrum. Fluorescence spectra were collected systematically both with increasing and with decreasing temperature to understand the effects of photochemistry as well as temperature on the fluorescence intensities of samples that were initially highly purified isomers. Emission spectra were corrected for the instrument response using a data file generated by a 200 W standard quartz tungsten-halogen filament lamp with spectral irradiance values traceable to NIST standards. For the display of spectra and the calculation of relative fluorescence yields, the emission spectra were converted to a wave-number scale and intensities were multiplied by  $\lambda^2$  to give relative emission intensities in photons/s  $cm^{-1}$ .<sup>30</sup>

## Results and Discussion

Figure 1 shows the HPLC of the hexadecaheptaene sample before and after photoisomerization. One- and two-dimensional NMR spectroscopy ( $^1H$ - $^1H$  COSY and  $^1H$ - $^1H$  NOESY)

(30) Lakowicz, J. R. *Principles of Fluorescence Spectroscopy*, 2nd ed.; Kluwer Academic, Plenum Publishers: New York, 1999.

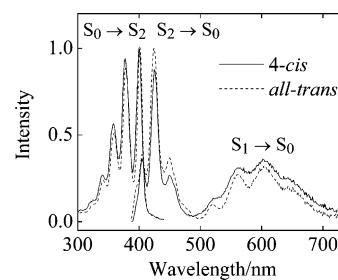


**Figure 2.** Absorption and fluorescence spectra of 4-*cis* (378 nm excitation) and *all-trans* (377 nm excitation) hexadecaheptaene in *n*-pentadecane at room temperature. The absorption spectra are normalized to their maximum values. Maximum absorbances of  $\sim 0.10$  minimized the effects of self-absorption. The fluorescence intensities have been corrected for the different room temperature absorbances of the two samples at the excitation wavelengths. Spectra were acquired with 1-nm band-passes.

identify the peak eluting at  $\sim 8.5$  min as the 4-*cis* isomer. This isomer dominates the products of the Wittig reaction, while the *all-trans* isomer is the major photochemical product. Irradiation of the pure *all-trans* isomer gives 4-*cis* hexadecaheptaene as the major photoproduct with the *all-trans* isomer dominating the photostationary state. The 4-*cis* and *all-trans* isomers thus are connected as major, but not exclusive, photoisomerization products of each other. Extended irradiation indicates that, in addition to photoisomerization, there are a variety of other photochemical and thermal processes that lead to irreversible degradation of the samples.

Collection of the 4-*cis* and *all-trans* fractions from the HPLC allows the comparison of their room temperature absorption and emission spectra in pentadecane (Figure 2). As noted in previous studies of a wide range of polyenes and carotenoids in solution,<sup>31–33</sup> the room-temperature fluorescence spectra and fluorescence quantum yields of the *cis* and *trans* samples are very similar. Following  $S_0$  ( $1^1A_g^-$ )  $\rightarrow$   $S_2$  ( $1^1B_u^+$ ) excitation, both isomers show dual emissions,  $S_2$  ( $1^1B_u^+$ )  $\rightarrow$   $S_0$  ( $1^1A_g^-$ ) and  $S_1$  ( $2^1A_g^-$ )  $\rightarrow$   $S_0$  ( $1^1A_g^-$ ), a signature of polyenes and carotenoids with intermediate conjugation lengths ( $N$  6–8).<sup>17,19,20,34,35</sup> In *n*-pentadecane, the emission and absorption spectra of the heptaenes exhibit sufficient vibronic resolution to allow the identification of the (0–0) bands, providing an accurate measure of the energies of the  $S_1$  ( $2^1A_g^-$ ) and  $S_2$  ( $1^1B_u^+$ ) states of these isomers.

The 77 K fluorescence and fluorescence excitation spectra of 4-*cis* hexadecaheptaene in *n*-pentadecane are presented in Figure 3. The high-resolution environment provided by the *n*-pentadecane matrix offers critical advantages in analyzing these spectra. The *n*-alkane mixed crystal selectively incorporates the polyene into a dominant substitutional site, providing well-defined, relatively homogeneous polyene–alkane interactions. This significantly decreases the inhomogeneous spectral broadening inherent to spectra obtained in solutions or low-

(31) Bautista, J. A.; Chynwat, V.; Cua, A.; Jansen, F. J.; Lugtenburg, J.; Gosztola, D.; Wasielewski, M. R.; Frank, H. A. *Photosynth. Res.* **1998**, *55*, 49–65.

(32) Andersson, P. A.; Takaichi, S.; Cogdell, R. J.; Gillbro, T. *Photochem. Photobiol.* **2001**, *74*, 549–557.

(33) Frank, H. A.; Desamero, R. Z. B.; Chynwat, V.; Gebhard, R.; van der Hoef, I.; Jansen, F. J.; Lugtenburg, J.; Gosztola, D.; Wasielewski, M. R. *J. Phys. Chem. A* **1997**, *101*, 149–157.

(34) Christensen, R. L. The electronic states of carotenoids. In *The Photochemistry of Carotenoids*; Frank, H. A., Young, A. J., Britton, G., Cogdell, R. J., Eds.; Kluwer Academic Publishers: Dordrecht, 1999; Vol. 8, pp 137–159.

(35) DeCoster, B.; Christensen, R. L.; Gebhard, R.; Lugtenburg, J.; Farhoosh, R.; Frank, H. A. *Biochim. Biophys. Acta* **1992**, *1102*, 107–114.

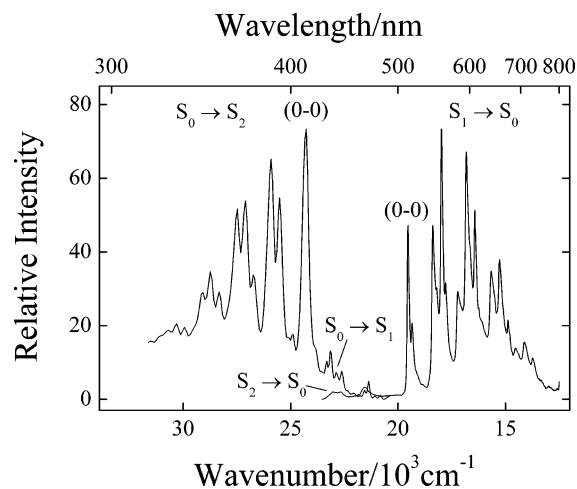


**Figure 3.** Fluorescence excitation and emission spectra of 4-*cis* hexadecaheptaene in *n*-pentadecane at 77 K. The fluorescence spectrum was obtained by exciting at 411 nm, and the fluorescence excitation spectrum was monitored at 594 nm. Maximum absorbances of  $\sim 0.10$  minimized the effects of self-absorption. Fluorescence intensities were corrected for the different room temperature absorbances of the two samples at the excitation wavelengths. Spectra were acquired with 1-nm band-passes.

temperature glasses. Although only the leading edge of the major 4-*cis* was collected from the HPLC (Figure 1), the samples no doubt contain small amounts of other isomers. However, the high-resolution environments provided by the mixed crystals provide enhanced selectivity in exciting and detecting emission from the dominant 4-*cis* component in fluorescence emission and excitation spectra. The use of *n*-alkane host crystals<sup>36,37</sup> has been exploited in several previous optical studies of simple polyenes,<sup>18,27,38–40</sup> including 2,4,6,8,10,12,14,16-octadecaheptaene, the longest linear polyene studied using low-temperature, high-resolution mixed-crystal techniques.<sup>40</sup>

The spectra of 4-*cis* hexadecaheptaene presented in Figure 3 exhibit well-resolved vibronic progressions in the  $S_0$  ( $1^1A_g^-$ )  $\rightarrow$   $S_2$  ( $1^1B_u^+$ ) absorption and the  $S_1$  ( $2^1A_g^-$ )  $\rightarrow$   $S_0$  ( $1^1A_g^-$ ) emission. As noted in previous studies on model polyenes,<sup>18,27,34,38–40</sup> these progressions are dominated by combinations of totally symmetric carbon–carbon single and carbon–carbon double bond stretches built on easily identified electronic origins. The low-temperature emission spectrum also shows features that can be identified with weak  $S_2$  ( $1^1B_u^+$ )  $\rightarrow$   $S_0$  ( $1^1A_g^-$ ) fluorescence. In addition, the spectra allow the identification of relatively sharp vibronic bands due to the weak  $S_0$  ( $1^1A_g^-$ )  $\rightarrow$   $S_1$  ( $2^1A_g^-$ ) transition on the low-energy tail of the strong  $S_0$  ( $1^1A_g^-$ )  $\rightarrow$   $S_2$  ( $1^1B_u^+$ ) absorption. This transition is considerably more difficult to detect and identify in the much broader spectra of polyenes and carotenoids in room temperature solutions and low-temperature glasses, illustrating another distinct benefit of the *n*-alkane matrices.

In contrast to the emission spectra obtained at room temperature, the 77 K fluorescence spectra (Figure 4) of the 4-*cis* and *all-trans* isomers in *n*-pentadecane are remarkably different. The  $S_2$  ( $1^1B_u^+$ )  $\rightarrow$   $S_0$  ( $1^1A_g^-$ ) emissions exhibit comparable intensities, with the *all-trans* isomer showing a small red shift in its

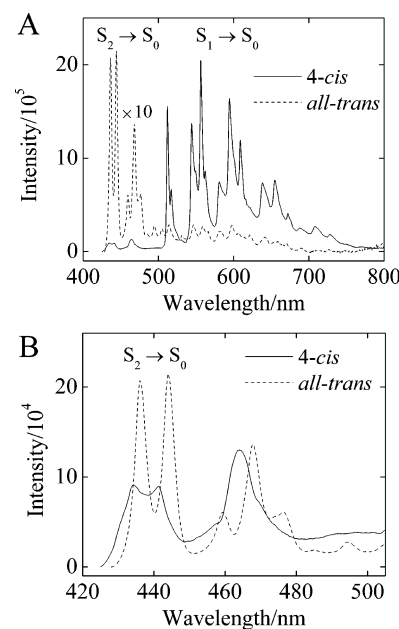


**Figure 4.** (A) Comparison of fluorescence spectra of 4-*cis* and *all-trans* hexadecaheptaene in *n*-pentadecane at 77 K. The relative fluorescence intensities have been corrected for the difference in the room temperature absorbances of the two samples. Emission spectra were obtained by exciting into the  $S_0 \rightarrow S_2$  (0–0) bands (414 nm for *all-trans*, 411 nm for 4-*cis*). (B) Expanded view of (A) showing the  $S_2 \rightarrow S_0$  fluorescence spectra of 4-*cis* hexadecaheptaene and *all-trans* hexadecaheptaene in *n*-pentadecane at 77 K. Emission band-passes were 1 nm for all spectra.

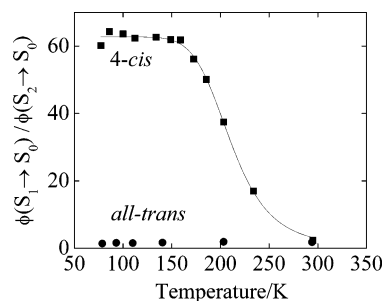


**Figure 5.** Ratios of integrated fluorescence yields ( $\phi(S_1 \rightarrow S_0)/\phi(S_2 \rightarrow S_0)$ ) for 4-*cis* (■) and *all-trans* (●) hexadecaheptaene as a function of temperature. The temperature dependence of the ratio for the 4-*cis* isomer was fit to eq 1 assuming that  $k_r$ ,  $k_{nr}$ , and  $\phi(S_2 \rightarrow S_0)$  are independent of temperature. The four-parameter fit (solid line) gives  $E_a = 4.3 \pm 1.4$  kcal.

somewhat better resolved spectrum (Figure 4B). On the other hand, at 77 K the  $S_1$  ( $2^1A_g^-$ )  $\rightarrow$   $S_0$  ( $1^1A_g^-$ ) emission of the 4-*cis* isomer is at least 20 times more intense than the  $S_1$  ( $2^1A_g^-$ )  $\rightarrow$   $S_0$  ( $1^1A_g^-$ ) emission of the *trans* isomer (Figure 4A). The dependence of the 4-*cis* emission yield on temperature is presented in Figure 5. In order to compensate for fluctuations in fluorescence intensities in the flowing  $N_2$  cryostat, we compare the ratio of integrated fluorescence intensities,  $\phi(S_1 \rightarrow S_0)/\phi(S_2 \rightarrow S_0)$ , for the two isomers. For the 4-*cis* isomer, the factor of  $\sim 15$  change in this ratio is almost entirely due to the increase in  $S_1$  ( $2^1A_g^-$ )  $\rightarrow$   $S_0$  ( $1^1A_g^-$ ) fluorescence upon cooling to 77 K. The corresponding ratio in the *all-trans* isomer shows a 2-fold decrease when the sample is cooled. It is important to note that the weak  $S_1$  ( $2^1A_g^-$ )  $\rightarrow$   $S_0$  ( $1^1A_g^-$ ) fluorescence observed for the *trans* isomer in part may be due to the photochemical production of highly fluorescent 4-*cis* and other *cis* impurities. The data indicated in Figures 4 and 5 thus may underestimate the true difference between the low-temperature

(36) Shpol'skii, E. V. *Sov. Phys. Usp.* **1962**, 5, 522–531.

(37) Shpol'skii, E. V. *Sov. Phys. Usp.* **1963**, 6, 411–427.

(38) Christensen, R. L.; Kohler, B. E. *J. Chem. Phys.* **1975**, 63, 1837–1846.

(39) Andrews, J. R.; Hudson, B. S. *J. Chem. Phys.* **1978**, 68, 4587–4594.

(40) Kohler, B. E.; Spangler, C.; Westerfield, C. J. *J. Chem. Phys.* **1988**, 89, 5422–5428.

$S_1$  ( $2^1A_g^-$ )  $\rightarrow$   $S_0$  ( $1^1A_g^-$ ) fluorescence yields of the pure 4-*cis* and pure *all-trans* isomers.

The *n*-alkane host offers a significant advantage for detecting the differences between  $S_1$  ( $2^1A_g^-$ )  $\rightarrow$   $S_0$  ( $1^1A_g^-$ ) fluorescence yields in the two isomers at low temperature. The *n*-pentadecane mixed crystal preserves the planar, symmetric ( $C_{2h}$ ) geometry of the *all-trans* heptaene, leading to relatively slow radiative decay for the symmetry-forbidden,  $S_1$  ( $2^1A_g^-$ )  $\rightarrow$   $S_0$  ( $1^1A_g^-$ ) transition. Furthermore, the *n*-pentadecane environment provides sufficient optical resolution to differentiate between emissions due to the 4-*cis* and the *all-trans* species (Figure 4). This is particularly important in distinguishing the weak emissions from the *trans* species from those of much more strongly emitting *cis* photochemical products. The differences between the fluorescence intensities of *cis* and *trans* samples are considerably less distinctive in the random environments provided by low-temperature glasses (data not shown), which produce a distribution of distorted *trans* polyenes, many of which do not have  $C_{2h}$  symmetry.

The current work recalls a previous controversy regarding the origin of the fluorescence signals (*cis* impurities versus the dominant *trans* species) in samples of cold, isolated octatetraene, the most highly studied and best-understood linear polyene. Buma et al.<sup>41</sup> assigned the isolated molecule,  $S_0$  ( $1^1A_g^-$ )  $\rightarrow$   $S_1$  ( $2^1A_g^-$ ) fluorescence excitation spectrum (obtained in a resonance-enhanced multiphoton ionization (REMPI) measurement) to a mono-*cis* isomer, arguing that the *trans* species would have insufficient oscillator strength for fluorescence detection. A subsequent study by Petek et al.,<sup>42</sup> on the high-resolution one- and two-photon fluorescence excitation spectra of octatetraene in supersonic jets, demonstrated that the oscillator strengths for the  $S_0$  ( $1^1A_g^-$ )  $\leftrightarrow$   $S_1$  ( $2^1A_g^-$ ) transitions in the *trans* isomer (induced by Herzberg–Teller vibronic coupling via low-frequency  $b_u$  promoting modes) were comparable to the corresponding oscillator strengths for *cis* isomers. This results in fluorescence intensities from the *cis* and *trans* isomers of isolated octatetraene that mirror their ground state abundances; i.e., the fluorescence spectra can be identified with the dominant *trans* isomer in typical samples. The identification of *all-trans* octatetraene as the dominant emitting species was confirmed by analysis of the rotationally resolved  $S_0$  ( $1^1A_g^-$ )  $\rightarrow$   $S_1$  ( $2^1A_g^-$ ) fluorescence excitation spectrum by Pfanstiel et al.<sup>43</sup> These experiments established that the absorbing and emitting states both had *all-trans*, planar geometries and also demonstrated that the  $S_0$  ( $1^1A_g^-$ )  $\leftrightarrow$   $S_1$  ( $2^1A_g^-$ ) electronic transitions gain their intensities via vibronic coupling with the  $S_2$  ( $1^1B_u^+$ ) state.

The work presented here shows that, in contrast to octatetraene, the 4-*cis* isomer of hexadecaheptaene has a much higher  $S_0 \leftrightarrow S_1$  oscillator strength than its *all-trans* counterpart. Under conditions where the *trans* isomer can be described by  $C_{2h}$  symmetry, e.g., in low-temperature *n*-pentadecane, the vibronically induced,  $S_1$  ( $2^1A_g^-$ )  $\rightarrow$   $S_0$  ( $1^1A_g^-$ ) radiative decay is relatively slow, and the fluorescence can be dominated by heptaenes with distorted, *s-cis* or *cis* conformations, even though these species may be present in relatively low concentrations.

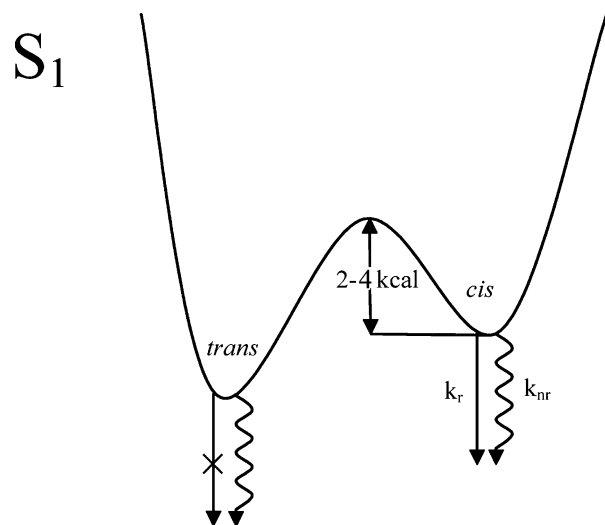


**Figure 6.** Schematic potential energy surface for hexadecaheptaene in the  $S_1$  ( $2^1A_g^-$ ) state.

The ability of *cis* isomers to dominate the fluorescence systematically increases with increasing conjugation length (manuscript in preparation).

The striking difference in temperature dependence of the fluorescence from the two isomers (Figure 5) leads to the simple, qualitative model presented in Figure 6. The thermodynamically favored *all-trans* isomer is connected to the 4-*cis* isomer by a relatively low-energy barrier in the  $S_1$  ( $2^1A_g^-$ ) state. Our preliminary photochemical studies (Figure 1) indicate that additional *cis* isomers also are accessible on the  $S_1$  ( $2^1A_g^-$ ) potential surface. Theoretical considerations also implicate *s-cis*, as well as distorted *trans* isomers on a complicated, multi-dimensional potential surface with many local minima, connected by relatively low barriers. However, since the 4-*cis* and *all-trans* isomers are the two major products of *all-trans* and 4-*cis* photoisomerization, we only consider these isomers in a much-simplified model (Figure 6). The lower energy, *all-trans* isomer dominates the photostationary state, a common theme in polyene and carotenoid photochemistry.<sup>44</sup> Our model (Figure 6) does not imply a mechanism for the isomerization; a detailed microscopic understanding of the chemistry would require additional experimental and theoretical work.

For the model presented in Figure 6, the  $S_1$  ( $2^1A_g^-$ )  $\rightarrow$   $S_0$  ( $1^1A_g^-$ ) fluorescence quantum yield for the 4-*cis* isomer can be approximated by

$$\phi(T) = k_r / (k_r + k_{nr} + Ae^{-E_a/RT}) \quad (1)$$

We assume that the radiative and nonradiative decay rates are independent of temperature and that the 4-*cis*  $\rightarrow$  *trans* isomerization proceeds over an activation barrier  $E_a$ . We also assume that the  $S_2$  ( $1^1B_u^+$ )  $\rightarrow$   $S_0$  ( $1^1A_g^-$ ) fluorescence yield does not depend on temperature in fitting the data presented in Figure 5 to eq 1. The resulting four-parameter fit (see Figure 5) yields an activation energy of  $4.3 \pm 1.4$  kcal and a pre-exponential factor ( $A$ ) of  $10^{10}$ – $10^{12}$  s<sup>-1</sup>. The fit is poorly determined; e.g., the parameters for the activation energy and pre-exponential factor are highly correlated with large uncertainties. The fits are heavily influenced by the high-temperature data points,

(41) Buma, W. J.; Kohler, B. E.; Shaler, T. A. *J. Chem. Phys.* **1992**, *96*, 399–407.

(42) Petek, H.; Bell, A. J.; Choi, Y. S.; Yoshihara, K.; Tounge, B. A.; Christensen, R. L. *J. Chem. Phys.* **1993**, *98*, 3777–3794.

(43) Pfanstiel, J. F.; Pratt, D. W.; Tounge, B. A.; Christensen, R. L. *J. Phys. Chem. A* **1999**, *103*, 2337–2347.

(44) Zechmeister, L. *Cis–trans isomeric carotenoids, vitamin A, and arylpolyenes*; Academic Press: New York, 1962.

which include the melting of the *n*-pentadecane crystal at 10 °C. In addition to the least-squares analysis, we also have employed simulations to explore the parameter space and to better understand the data and the model (eq 1). The determination of relative fluorescence yields as a function of temperature on samples undergoing photoisomerization is particularly challenging, especially for weakly emitting species. In spite of the limitations of both the model and the data, the parameters extracted from eq 1 are consistent with thermally activated, 4-*cis* → *trans* isomerization in the  $S_1$  state.

An identical model was postulated to account for the temperature dependence of  $S_1$  lifetimes of *cis* and *trans* octatetraenes in different *n*-alkane solvents.<sup>45</sup> The temperature-dependences of the octatetraene  $S_1$  lifetimes between 77 K and room temperature are comparable to the data presented in Figure 5 and also were interpreted in terms of a thermally activated *cis* [→] *trans* isomerization in  $S_1$  with pre-exponential factors of  $10^{10}$ – $10^{12}$  s<sup>-1</sup> and activation energies of a few kcal/mol.<sup>45,46</sup> For example, analysis of lifetime data indicated an  $S_1$  barrier of 1.1 kcal for the isomerization of *cis,trans*-1,3,5,7-octatetraene to the *all-trans* isomer<sup>47</sup> and 2.5 kcal for the reverse process.<sup>45</sup> The connections between the temperature dependence of the fluorescence lifetimes of octatetraene isomers and the fluorescent quantum yield data presented in Figure 5 with excited-state isomerizations are buttressed by the temperature dependence of the photochemical quantum yields for *trans* → *cis* isomerizations in *all-trans* retinal. These studies indicate activation barriers of 1.6–3.2 kcal, depending on the solvent and the *cis* isomer formed.<sup>48</sup> It also is important to note that the barriers to C=C isomerization in the  $S_1$  state are comparable to those for isomerization of carbon–carbon single bonds in polyene ground states.<sup>46,49</sup> This reflects the significant rearrangement of the C–C and C=C  $\pi$ -bond orders in going from the ground to the  $S_1$  state.<sup>50</sup>

The low thermal barrier associated with the >20-fold increase in the  $S_1$  ( $2^1A_g^-$ ) →  $S_0$  ( $1^1A_g^-$ ) fluorescence intensity with decreasing temperature cannot be explained by isomerization on the ground state  $S_0$  ( $1^1A_g^-$ ) potential energy surface. It also is not consistent with isomerization in the short-lived  $S_2$  state ( $1^1B_u^+$ ). If that were the case, we would expect a substantial change with temperature in the quantum yield of  $S_2$  ( $1^1B_u^+$ ) →  $S_0$  ( $1^1A_g^-$ ) emission, which is not observed. The increase in the ratio,  $\phi(S_1 \rightarrow S_0)/\phi(S_2 \rightarrow S_0)$ , for the 4-*cis* isomer, thus is almost entirely due to the increase in  $S_1$  ( $2^1A_g^-$ ) →  $S_0$  ( $1^1A_g^-$ ) fluorescence upon cooling. Furthermore, in solutions, *trans* ↔ *cis* isomerization in  $S_1$  ( $2^1A_g^-$ ) must compete with rapid nonradiative processes, which tend to dominate the excited-state decays of longer polyenes and carotenoids.<sup>20</sup>

The *all-trans* heptaene  $S_1$  →  $S_0$  fluorescence yield shows a 2-fold increase with temperature (Figure 5), suggesting that it crosses over a barrier in  $S_1$  to a more fluorescent species. It is tempting to ascribe this weak emission as due to adiabatic conversion to 4-*cis* heptaene in our simple model. This would account for the rather similar room-temperature fluorescence spectra of the *all-trans* and 4-*cis* species (Figure 2) and the fact

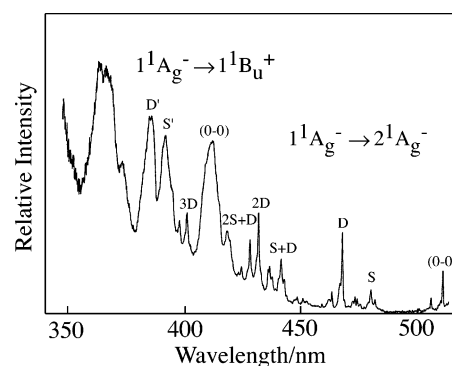


**Figure 7.** Fluorescence excitation spectra ( $1^1A_g^- \rightarrow 2^1A_g^-$  and  $1^1A_g^- \rightarrow 1^1B_u^+$ ) of 4-*cis*-2,4,6,8,10,12,14-hexadecaheptaene in 10 K *n*-pentadecane. Fluorescence was detected at 560 nm. Vibronic features labeled with S and D (and S' and D') indicate combinations of C–C and C=C symmetric stretching modes. This spectrum was obtained on a more concentrated sample than that used for the excitation spectrum presented in Figure 3. This amplifies the  $1^1A_g^- \rightarrow 2^1A_g^-$  absorption. The excitation spectrum is not corrected for the wavelength dependence of the excitation system (figure adapted from Figure 3 of ref 18).

that the 4-*cis* isomer is the dominant photoisomerization product of *all-trans*-hexadecaheptaene. However, the very small fluorescence yields of the *all-trans* isomer at all temperatures make it difficult to identify its fluorescence with a particular asymmetric species. Adiabatic pathways to other *cis* isomers, distorted *trans* conformers, as well as isomerization upon relaxation to the ground state all could induce fluorescence in samples of pure,  $C_{2h}$ , *all-trans* hexadecaheptaene. It thus is much easier to make the case for 4-*cis* → *all-trans* adiabatic  $S_1$  conversion than for the reverse process.

The potential energy diagram presented in Figure 6 is similar to that proposed by de Weerd et al.<sup>51</sup> based on subpicosecond dynamics studies of *all-trans*  $\beta$ -carotene. However, those authors suggested that  $\beta$ -carotene became distorted in the  $S_2$  ( $1^1B_u^+$ ) state and relaxed back to the *all-trans* configuration upon decaying to  $S_1$  ( $2^1A_g^-$ ). This is not the case for hexadecaheptaene, and other investigators have argued that conformational twisting occurs in  $S_1$  ( $2^1A_g^-$ ) in  $\beta$ -carotene<sup>52</sup> and other carotenoids.<sup>52–54</sup>

The relatively large oscillator strength for the  $S_0$  ( $1^1A_g^-$ ) ↔  $S_1$  ( $2^1A_g^-$ ) transition in 4-*cis* hexadecaheptaene is confirmed by our ability to detect the  $S_0$  ( $1^1A_g^-$ ) →  $S_1$  ( $2^1A_g^-$ ) transition in the high-resolution fluorescence excitation spectrum (Figure 7). The ~4700 cm<sup>-1</sup> gap between the  $1^1B_u^+$  and  $2^1A_g^-$  states provides a wide window for observing the vibronic development of the  $2^1A_g^-$  vibronic states built on the electronic origin (0–0) at 512 nm. Note also the coincidence between the 512 nm (0–0) bands in the  $S_0$  ( $1^1A_g^-$ ) →  $S_1$  ( $2^1A_g^-$ ) excitation spectrum (Figure 7) and the  $S_1$  ( $2^1A_g^-$ ) →  $S_0$  ( $1^1A_g^-$ ) emission spectrum (Figure 3). The overlap between electronic origins and the relatively strong  $S_0$  →  $S_1$  absorption indicate a symmetry-allowed electronic transition, as expected for the 4-*cis* isomer. A large  $S_0$  ↔  $S_1$  oscillator strength explains the considerable enhancement in the 4-*cis*  $S_1$  →  $S_0$  fluorescence yield compared

(45) Kohler, B. E.; Mitra, P.; West, P. *J. Chem. Phys.* **1986**, *85*, 4436–4440.

(46) Kohler, B. E. *Chem. Rev.* **1993**, *93*, 41–54.

(47) Ackerman, J. R.; Kohler, B. E. *J. Am. Chem. Soc.* **1984**, *106*, 3681–3682.

(48) Waddell, W. H.; Chihara, K. *J. Am. Chem. Soc.* **1981**, *103*, 7389–7390.

(49) Ackerman, J. R.; Kohler, B. E. *J. Chem. Phys.* **1984**, *80*, 45–50.

(50) Schulten, K.; Ohmine, I.; Karplus, M. *J. Chem. Phys.* **1976**, *64*, 4422–4441.

(51) de Weerd, F. L.; van Stokkum, I. H. M.; van Grondelle, R. *Chem. Phys. Lett.* **2002**, *354*, 38–43.

(52) Kosumi, D.; Yanagi, K.; Nishio, T.; Hashimoto, H. M. Y. *Chem. Phys. Lett.* **2005**, *408*, 89–95.

(53) Billsten, H. H.; Pan, J.; Sinha, S.; Pascher, T.; Sundström, V.; Polívka, T. *J. Phys. Chem. A* **2005**, *109*, 6852–6859.

(54) Pendon, Z. D.; Gibson, G. N.; van der Hoef, I.; Lugtenburg, J.; Frank, H. A. *J. Phys. Chem. B* **2005**, *109*, 21172–21179.

with that associated with the symmetry forbidden transition of the *all-trans* isomer. The excitation spectra for both the  $S_0 \rightarrow S_1$  and  $S_0 \rightarrow S_2$  absorptions show the classic pattern of vibronic intensities built on combinations of carbon–carbon single and double bond symmetric stretching modes. The vibronic spectrum shown in Figure 7 previously was analyzed by Simpson et al. and assigned to the *all-trans* isomer.<sup>18</sup> However, our current work shows that the vibronic states observed are due to 4-*cis* hexadecaheptaene.

## Conclusions

The results presented here require a reinterpretation of fluorescence experiments previously carried out on *all-trans* isomers of longer polyenes and of related carotenoids. Several previous studies of longer linear polyenes ( $N > 4$ ) have assigned  $S_1 \rightarrow S_0$  fluorescence signals to *all-trans* isomers. Examples include the high-resolution work of Simpson et al. on hexadecaheptaene<sup>18</sup> and of Kohler et al. on octadecaheptaene.<sup>40</sup> The excitation and fluorescence spectra were assigned to *all-trans* species, but our work indicates that the  $S_1 \rightarrow S_0$  emission spectra of these longer polyenes most likely are due to *cis* isomers, present as impurities or formed as photochemical products in the  $S_1$  state. This is a significant finding, given that existing theoretical work (almost all on simple *all-trans* polyenes)<sup>4,5,55,56</sup> has been compared with experimental work on what now must be assigned to *cis* species. Rapid isomerization in  $S_1$  ( $2^1A_g^-$ ) explains the typically small differences between the  $S_1$  ( $2^1A_g^-$ )  $\rightarrow$   $S_0$  ( $1^1A_g^-$ ) emission spectra and quantum yields of *cis* and *trans* systems in room temperature solutions. The almost negligible  $S_1$  ( $2^1A_g^-$ )  $\rightarrow$   $S_0$  ( $1^1A_g^-$ ) fluorescence yields from  $C_{2h}$ , *trans* species and the relatively low resolution of solution and glass spectra prohibit a ready distinction between emissions due to *trans* isomers from those due to *cis* impurities or from *trans* molecules with conformational distortions that relax the rigorous selection rules. We thus conclude that, except for the very detailed studies of *all-trans* octatetraene, *previous reports of  $S_1$  emissions from all-trans,  $C_{2h}$  polyenes and carotenoids most likely are due to less symmetric species.* These species may be present as ground state impurities, including photochemical products, or formed in the  $S_1$  ( $2^1A_g^-$ ) state following the excitation of *all-trans* polyenes.

Our results suggest that steady-state fluorescence experiments and time-resolved measurements, e.g.,  $S_1 \rightarrow S_N$  transient absorption experiments, detect different distributions of  $S_1$  ( $2^1A_g^-$ ) conformers and geometric isomers, even for samples with a single, *all-trans*, ground state structure. For example, the elegant  $S_1$  ( $2^1A_g^-$ )  $\rightarrow$   $S_2$  ( $1^1B_u^+$ ) absorption experiments of Polívka et al.<sup>57</sup> on several *all-trans* carotenoids, including spheroidene, zeaxanthin and violaxanthin, were compared with the transition energies for the strongly allowed  $S_0$  ( $1^1A_g^-$ )  $\rightarrow$   $S_2$  ( $1^1B_u^+$ ) absorptions. The energy difference in the electronic origins ((0–0) bands) of these two symmetry-allowed transitions yields the  $S_1$  ( $2^1A_g^-$ ) energy. However,  $S_1$  electronic energies obtained in this manner were found to be consistently 500–

1000  $\text{cm}^{-1}$  lower than those from the fluorescence measurements. This is in accord with the model presented in Figure 6. Fluorescence from these samples is from higher energy, distorted *trans* and/or *cis* carotenoids with  $S_1 \leftrightarrow S_0$  oscillator strengths and radiative decay rates that are sufficiently large to compete with the rapid ( $\sim 10$  ps) nonradiative decays in these molecules. It should be noted that Polívka et al.<sup>58,59</sup> suggested a similar model, though did not invoke isomerization, to explain the discrepancies between their results and the  $S_1$  ( $2^1A_g^-$ ) energies estimated by fluorescence techniques. Another conclusion from the current studies is that, at least for longer polyenes and related carotenoids, “forbidden” electronic transitions for molecules with  $C_{2h}$  symmetries will be very difficult to detect. Optical techniques that exploit the selection rules for allowed transitions, e.g.,  $S_1$  ( $2^1A_g^-$ )  $\rightarrow$   $S_2$  ( $1^1B_u^+$ ) absorption, thus have obvious advantages in accurately locating the excited electronic energy levels of *trans* polyenes and carotenoids.

The low-energy barriers to isomerization and conformational distortion in  $S_1$  ( $2^1A_g^-$ ) are consistent with significant rearrangements of the ground state C–C and C=C bond orders relative to the changes in  $S_2$  ( $1^1B_u^+$ ) and other low-energy excited states.<sup>3–5</sup> This transposition of  $\pi$ -bond orders is a hallmark of polyene electronic structure and explains the unique ability of  $S_1$  states to promote rapid isomerization. Low barriers to isomerization and conformational change also may account for the complex kinetics of  $S_2$  ( $1^1B_u^+$ )  $\rightarrow$   $S_1$  ( $2^1A_g^-$ ) nonradiative decay in carotenoids. As mentioned previously, Cerullo et al.<sup>10</sup> postulate the existence of an excited electronic state ( $S_x$ ) between  $S_2$  ( $1^1B_u^+$ ) and  $S_1$  ( $2^1A_g^-$ ) that decays on an  $\sim 100$  fs time scale, and van Grondelle et al.<sup>11</sup> hypothesize that additional short-lived electronic singlet states ( $S^*$  and  $S^\ddagger$ ) provide alternate routes for internal conversion from  $S_2$ . The current work strongly suggests that at least some of these proposed singlet electronic states instead may be manifestations of nonradiative decay on complicated  $S_1$  ( $2^1A_g^-$ ) potential surfaces. These surfaces provide multiple pathways for the zero-point level of  $S_2$  ( $1^1B_u^+$ ) to change its geometry to arrive at vibrationally relaxed, thermally equilibrated  $S_1$  ( $2^1A_g^-$ ).

**Acknowledgment.** We thank Tomáš Polívka and Robert Birge for fruitful discussions. R.L.C. has been supported by the Bowdoin College Kenan and Porter Fellowship Programs and acknowledges funding from NSF-ROA (MCB-0314380 to HAF) and the Petroleum Research Fund, administered by the American Chemical Society. R.L.C. also was supported in this work while serving at the National Science Foundation. This research is supported in the laboratory of HAF by the National Institutes of Health (GM-30353) and the University of Connecticut Research Foundation. H.H. and R.F. acknowledge grants-in-aid (No. 17204026 and 17654083) from the Japanese Ministry of Education, Culture, Sports, Science and Technology. H.H. and R.F. also acknowledge financial support from the Strategic International Cooperative Program of the Japan Science and Technology Agency. We also acknowledge the helpful comments of one of the referees in clarifying our understanding of the role of adiabatic photoisomerization in hexadecaheptaene.

**Supporting Information Available:**  $^1\text{H}$  chemical shifts and correlations of  $^1\text{H}$ – $^1\text{H}$  COSY and  $^1\text{H}$ – $^1\text{H}$  NOESY of 4-*cis* hexadecaheptaene. This material is available free of charge via the Internet at <http://pubs.acs.org>.

JA0609607

- (55) Tavan, P.; Schulten, K. *J. Chem. Phys.* **1979**, *70*, 5407–5413.  
(56) Head-Gordon, M.; Rico, R. J.; Oumi, M.; Lee, T. *J. Chem. Phys. Lett.* **1994**, *219*, 21–29.  
(57) Polívka, T.; Herek, J. L.; Zigmantas, D.; Akerlund, H. E.; Sundström, V. *Proc. Natl. Acad. Sci. U.S.A.* **1999**, *96*, 4914–4917.  
(58) Polívka, T.; Zigmantas, D.; Frank, H. A.; Bautista, J. A.; Herek, J. L.; Koyama, Y.; Fujii, R.; Sundström, V. *J. Phys. Chem. B* **2001**, *105*, 1072–1080.  
(59) Polívka, T.; Sundström, V. *Chem. Rev.* **2004**, *104*, 2021–2071.